Mechanical and corrosion behaviors of developed copper-based metal matrix composites

IOP Conf. Series: Materials Science and Engineering **330** (2018) 012021 doi:10.1088/1757-899X/330/1/012021

Mechanical and corrosion behaviors of developed copper-based metal matrix composites

Manvandra Kumar Singh[1*], Rakesh Kumar Gautam[1], Rajiv Prakash[2] and Gopal Ji[2]

[1]Department of Mechanical Engineering, Indian Institute of Technology (Banaras Hindu University), Varanasi-221005, India
[2]School of Materials Science and Technology, Indian Institute of Technology (Banaras Hindu University), Varanasi-221005, India

*Corresponding author E-mail: mksingh.rs.mec13@itbhu.ac.in

Abstract. This work investigates mechanical properties and corrosion resistances of cast copper-tungsten carbide (WC) metal matrix composites (MMCs). Copper matrix composites have been developed by stir casting technique. Different sizes of micro and nano particles of WC particles are utilized as reinforcement to prepare two copper-based composites, however, nano size of WC particles are prepared by high-energy ball milling. XRD (X-rays diffraction) characterize the materials for involvement of different phases. The mechanical behavior of composites has been studied by Vickers hardness test and compression test; while the corrosion behavior of developed composites is investigated by electrochemical impedance spectroscopy in 0.5 M H_2SO_4 solutions. The results show that hardness, compressive strength and corrosion resistance of copper matrix composites are very high in comparison to that of copper matrix, which attributed to the microstructural changes occurred during composite formation. SEM (Scanning electron microscopy) reveals the morphology of the corroded surfaces.

1. Introduction

Copper contains high electrical conductivity, thermal conductivity and ductility as well as good corrosion resistance in various media [1, 2]. Due to these effective reasons, copper and its alloys are widely utilized in many engineering and industrial applications like automobiles, houses, sanitary system (underground or under sea drinking water pipes), electronic and electrical devices, and lead frame materials for integrated circuits [3, 4]. In spite of having all the above listed properties, copper and alloys rapidly lose their mechanical strength and corrosion resistance in some aggressive environments [5-7]. This can cause complete failure of the copper-based appliances, which may lead to adverse circumstances. Hence, it becomes important to improve their anti corrosion and mechanical strength in active working environments [8-10]. One of the most effective methods adapted for enhancing the mechanical strength and corrosion resistance of copper is alloying [11, 12]. Due to the alloying effect, the mechanical properties of copper improve; and the span of safe operation period increases [13-15]. The effects of alloying with the different elements on the properties of copper have been well studied by various scientists [16-18].

The first aim of the present work is to investigate the changes in mechanical properties of copper due to alloying with WC particles (micro and nano size). The second aim of this work is to study the corrosion inhibition behavior of copper matrix composites in 0.5 M H_2SO_4 solutions. Ceramic materials, especially carbides [19-21], are widely used as reinforcement particles in metal matrix composites. However, the ceramic particles have the natural tendency to generate micro cracks in the composites due to poor wettability with the matrix metal [22]. Hence, we have selected both micro and nano size (for better dispersion) WC powder as reinforcement particles in making of copper matrix composites. WC reinforced copper matrix composites are made by stir casting technique. Hardness, compressive strength and corrosion behavior of prepared Cu-WC composites have been investigated by Vickers hardness test, compression test and electrochemical impedance spectroscopy (EIS) techniques. The results show significant improvement in mechanical and anti corrosion strength of copper due to alloying with WC, which justify alloying of copper with WC particles.

2. Materials and Methods

2.1. Preparation of micro and nano copper composites

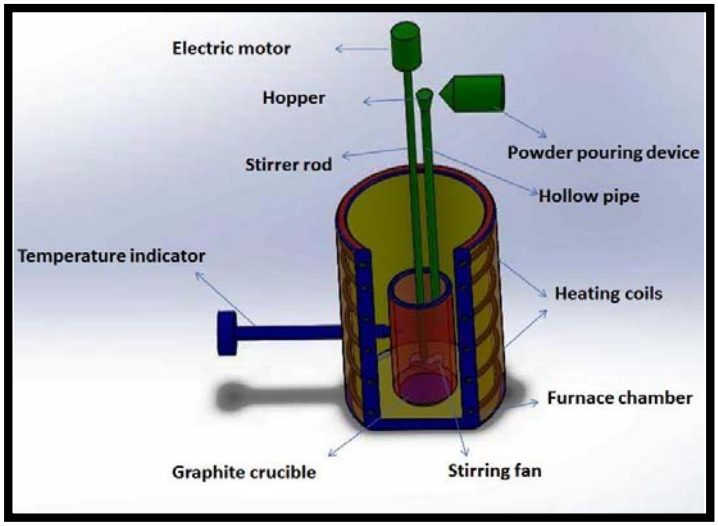

Figure 1. Schematic diagram showing details of a stir- casting process

Matrix material (copper of 99.5 % purity) was purchased from the local shop at Varanasi, India. WC powder (HIMEDIA with 98.0 % assay, micro size) and chromium powder (LOBA CHEMIE with 99.0 % assay) were bought from local chemical supplier. Micro size particles of WC were ball milled for a long period and thus converted into nano size particles. To prepare micro and nano composites of copper and WC, firstly 1 wt % of WC micro and nano powder, 2.0 wt % of chromium (Cr) and rest copper (in rod from) were weighed. Then, a graphite crucible that contains small pieces of copper rod was kept in the electric furnace. The furnace temperature was raised up to 1200º C. At this high temperature copper melts; and then dry micro and nano WC particles were poured separately into crucibles followed by addition of Cr, with the help of powder pouring system (Figure 1). During pouring of powders, the stirrer was rotated at very slow speed of 50rpm; however, the speed of stirrer was increased to 400 rpm for 10 minutes after completion of the pouring process. Afterwards, the furnace was shutdown and crucible was taken out from the furnace. Thus, prepared materials were poured into permanent

moulds and left for cooling in air. Afterwards, Cu-WC composites were abraded by 1/0 to 6/0 grade of emery paper sequentially and cleaned by acetone followed by washing with double distilled water. Thus, prepared composites were used for further characterizations.

2.2 XRD analysis of nano WC powder and Cu-WC composite materials

X-ray diffraction patterns for powder samples of Cu, WC and Cu-WC composites were obtained by 18 kW anode powder X-ray diffractometer, Rigaku, Japan in the range of 20º to 80º with Cu-Kα radiation at a scan rate of 3º per minute. The powder samples of Cu and Cu-WC composite were obtained by scraping them with a file. Thus, obtained powders were used for XRD analysis.

2.3 Microstructural examination of copper and copper-WC composites

The microstructural analysis of the copper and copper matrix micro and nano composites was performed on the optical microscope of De-winter Optical Inc, India. Prior to investigation, the test specimen were prepared by grinding them with the emery papers of 200, 400, 600, 800, 1200 and 1600 grit number. The specimens were first grinded with the emery paper of 200 grit number for 10 minutes. Afterwards, the abrading of the specimen was done for 10 minutes with the 400 grit number emery paper at 90º angle to the direction of grinding the specimen with 200 grit number emery paper. The same procedure was followed in grinding of the specimen with the emery paper of 600, 800, 1200 and 1600 grit number. After completion of the grinding process, the specimens were polished by the velvet cloths having Brasso as a polishing agent. After polishing, the specimens were washed under the running tap water and dried with the hot air to remove the stains from the specimen's surface. In the last step, the specimens were partially dipped in the ferric chloride solution (etchant) for 6 seconds and drawn out afterwards. Thus prepared specimens were used for the microstructural analysis.

2.4 Vickers micro hardness test

The Vickers micro hardness test method included indentation of copper and composite materials (specimen dimension: 15 mm×15 mm×2 mm) with a diamond indenter. The indenter was in the shape of pyramid with square base and having an angle of 136º between opposite faces. The test samples were subjected to a load of 0.5 kgf for 10 seconds. Due to application of load, an impression of indenter appeared on sample's surfaces. The two diagonals of this indentation (d_1 and d_2) were measured with the help of a microscope and arithmetic of these two used in the formula. Vickers hardness (HV) values of the samples calculated from the following equation:

$$HV = \{2F\sin(136º/2)\}/d^2 \quad \text{---------- Eq. 1}$$

Where, F is Load in kgf and d correspond to arithmetic mean of the two diagonals d_1 and d_2 in mm.

2.5 Compression test

The compressive strengths of copper and composite materials were investigated by universal testing machine (UTM). For compression test, the specimens were prepared in cylindrical form that was 20 mm in length and 10 mm in diameter. The test specimens were compressed with the help of UTM until buckling deformation of samples. The load at which samples started to deform, or crack appeared on sample's surface, was designated as critical compressive load. Compressive strengths of samples were obtained by dividing critical compressive load by area of samples.

2.6 Corrosion testing and surface morphology analysis

Corrosion testing of copper and copper-WC composites (sample surface area- 1 cm^2) was performed by electrochemical impedance spectroscopy (EIS) technique with help of an electrochemical workstation, CH Instrument (USA), in a three electrode glass cell. In this cell assembly, platinum foil (1 cm×1 cm) as counter electrode, Ag/AgCl as reference electrode and test samples as working electrodes were employed. The EIS spectra were obtained at open circuit potentials by applying 5 mV excitation signals in the frequency range of 10 mHz to 100 kHz [23-25]. The active parameters of corrosion process were obtained by fitting of Nyquist plots with ZSim software (version 3.20).

The effect of alloying on corrosion behavior of copper was monitored by SEM microscope of Carl Zesis, model- Supra 40, made in Germany. The samples of 1 cm^2 surface area were immersed in beakers having 100 mL of 0.5 M H_2SO_4 solutions for 2 hours. Afterwards, the specimens were drawn out; washed with double distilled water; wiped with a tissue paper and dried in a hot oven at 30° C for 10 minutes. Thus, prepared samples were investigated for the surface morphology changes in copper due to alloying. For a comparison, SEM images of the unexposed samples of copper and composites were captured.

3. Results and Discussion

3.1. XRD analysis

3.1.1. XRD analysis of high energy ball milled WC powder.

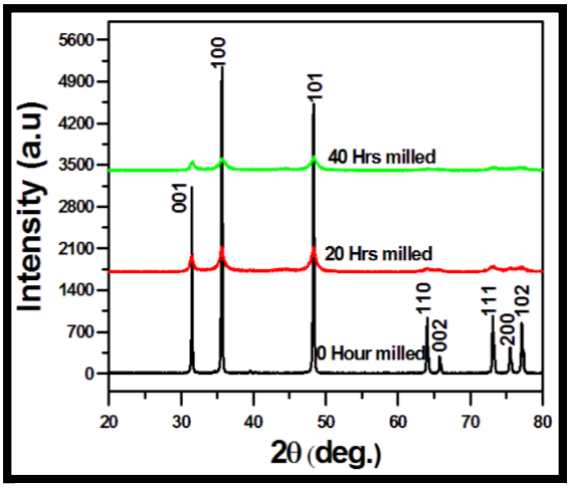

Figure 2. XRD plots of high-energy ball milled WC powder

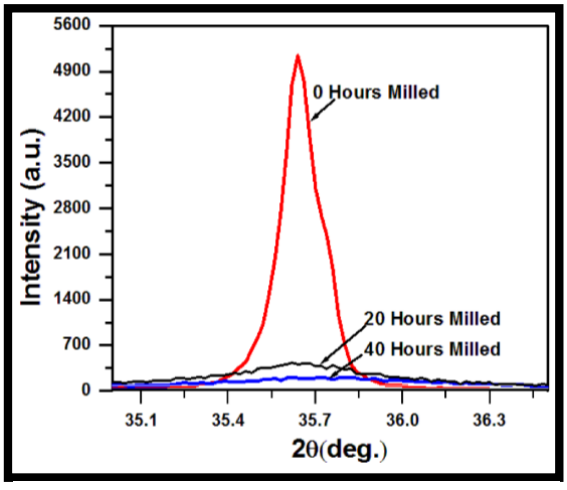

Figure 3. Peak broadening in XRD spectrum of milled WC powder

X-rays diffraction patterns of high-energy ball milled WC powder at zero hour (pure WC powder), 20 hours and 40 hours are shown in Figure 2. From analysis of XRD patterns, it is observed that peak intensities of tungsten powder decreased with the period of ball milling. However, broadening of peak occurred with the time of ball milling. This fact indicated that WC powder is converted in nano size particles from micro size powder particles. This statement could be supported by the fact that XRD peaks became broader due to reduction in particle size [26] (Figure 3). Furthermore, the size of WC particles is calculated by Scherrer formula [27].

$$D = 0.9\lambda/B \cos\theta \quad \text{---------- Eq.2}$$

Where, D is crystallite size, λ is the wavelength of the X-ray radiation, B is the peak width at half of maximum intensity and θ correspond to the Bragg angle. The size of WC particles after 40 hours ball milling calculated from scherrer formula is 19 nm.

3.1.2 XRD analysis of composite materials. Figure 4 shows XRD patterns of copper and Cu-WC micro composite. From analysis of Figure 4, it is observed that there were some common peaks in XRD patterns of WC and copper. XRD peaks of WC are absent in Figure 4 because they have already shown in Figure 2; however, we have illustrated some characteristic peaks of WC in text form. Figure 4 revealed that intensities of XRD peaks of Cu-WC composite are higher than peak intensities of WC (Figure 2). In addition, these peaks appeared in XRD pattern of copper. Hence, it could be concluded based on above-mentioned information that Cu-WC composite is successfully prepared. Here, the x-rays diffraction pattern of the Cu-WC nano composite has not been shown because the reinforcing element is same, i.e., WC. Also, only difference between Cu-WC micro and nano composite is size of WC, which will not affect XRD peak positions very much (Figure 2).

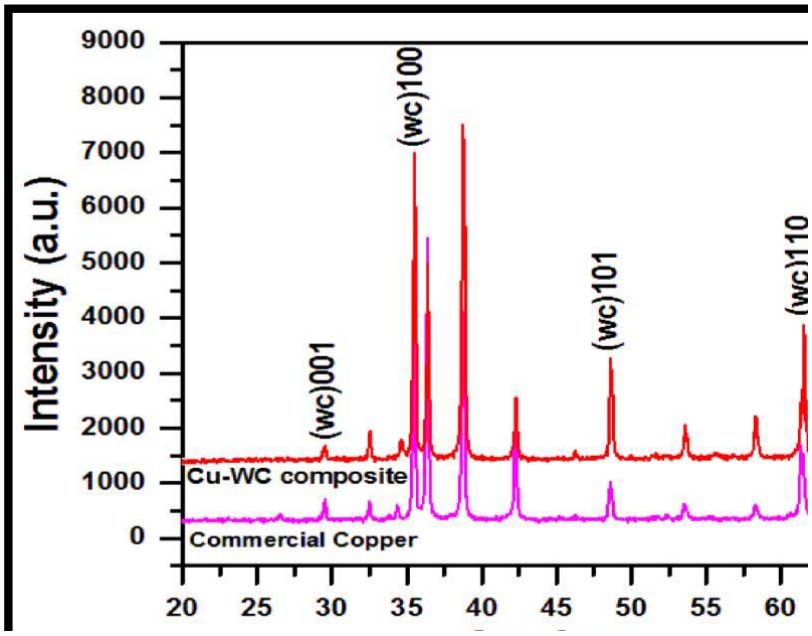

Figure 4. XRD plot of commercial copper and micro composite XRD plot of commercial copper and micro composite materials

3.2 Micro structural analysis

The optical micrographs of as-cast Cu, Cu-WC micro composite and Cu-WC nano composite are shown in Figure 5. A quick analysis of Figure 5a revealed that there are some pores present on the copper surface, which could be considered as a casting defect. Figure 5b showed that WC particles (black) are well dispersed in copper matrix (white); however, the WC particle size is not uniform. On the other hand, Figure 5c revealed that nano WC particles are more uniform in size and finely dispersed in copper matrix. To explain the contributions of nano and micro WC particles in Cu matrix in a better way, the microstructures of copper and composites (Figure 5) are studied and shown in Figure 6. It is clear through analysis of Figure 6 that WC particles assisted in colonization of copper grains. However, finer grains and a dense structure are

achieved using nano WC particles in comparison to micro WC particles; which demonstrated that better reinforcement could be achieved with nano WC particles.

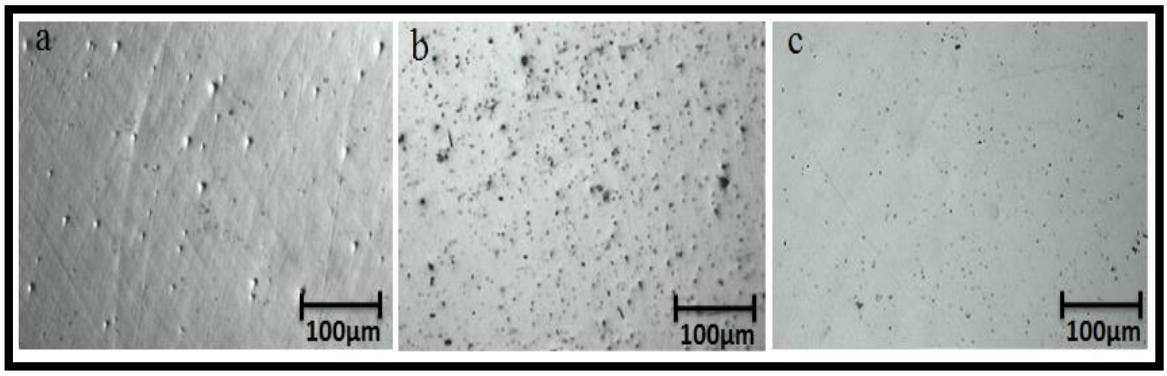

Figure 5. Optical images showing microstructure of **(a)** cast Cu, **(b)** Cu-WC micro composite and **(c)** Cu-WC nano composite just before etching

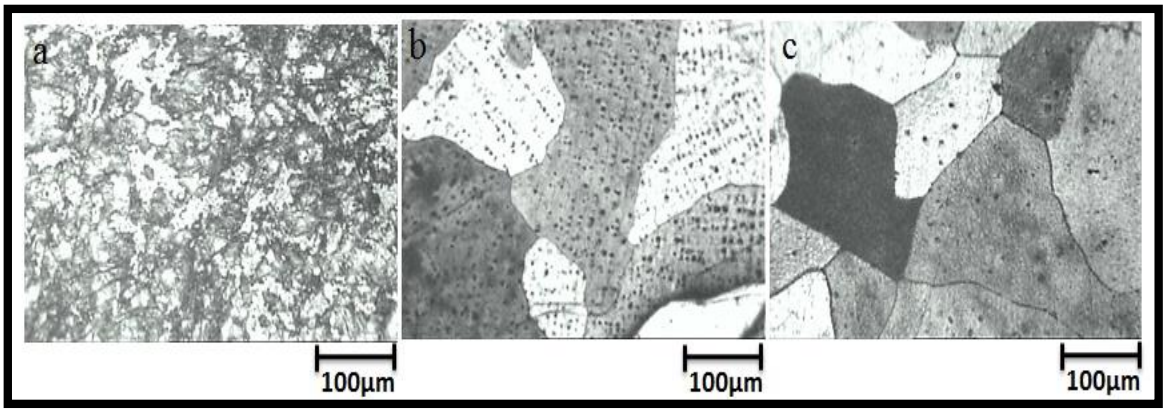

Figure 6. Optical images showing microstructure of **(a)** cast Cu, **(b)** Cu-WC micro composite and **(c)** Cu-WC nano composite obtained after etching

3.3. Vickers hardness test

Vickers hardness tests of copper, copper micro composite and copper nano composite are performed at 0.5 kgf load; and the results are shown in Figure 7. Analysis of Figure 7 revealed that the hardness values of nano and micro Cu-WC composites were higher than the hardness value of copper, which clearly indicated that addition of micro and nano WC particles enhanced hardness of matrix material (copper). However, hardness of copper-WC nano composite is the highest among all tested materials. This fact could be effectively described with the help of Hall-Petch relationship. According to this, distribution of filler material in matrix material increases with reduction in particle size of metals, which causes increase in hardness value of composite materials [28]. The grain size is also an important parameter, which has strong influence on metal strength. This is due to different orientation of adjacent grains and high lattice disorder characteristics of these regions, which prevents dislocation to move in a continuous slip plane [29].

3.4. Compression test

Compression tests of copper and composite materials have been executed on universal testing machine and results are shown in Figure 8. A careful inspection of Figure 8 revealed that compressive strengths of copper composites are greater than that of copper alone. However, the compressive strength of Cu-WC nano composite is the highest among all studied materials in this work. Such an increase in the compressive strength of both micro and nano composite of Cu and WC might be occurred due to the combined effects of load transfer, Hall-Petch strengthening and Orowan strengthening. Compressive strength of composite materials might increase by strengthening of the base material due to the load transfer from the soft and compliance matrix to the stiff and hard ceramic WC particles under an applied external load [30-32]. Fine distribution of the ceramic WC in copper matrix might be one of the reasons for enhancement of compressive strength of both micro and nano composite materials [27]. In addition, the strength of composite materials might increase due to pining up of dislocations crossing over WC particles under external load [29].

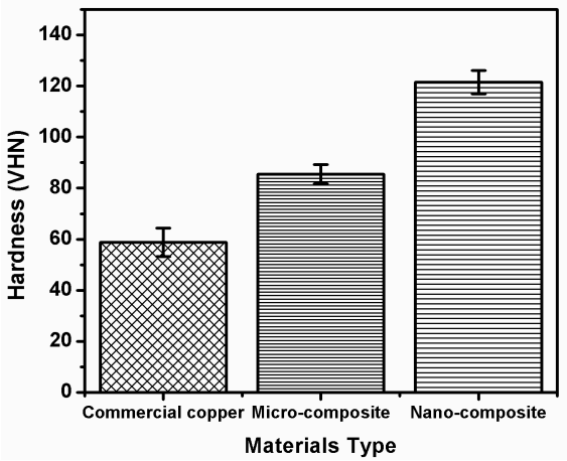

Figure 7. Hardness (VHN) of copper and copper composites

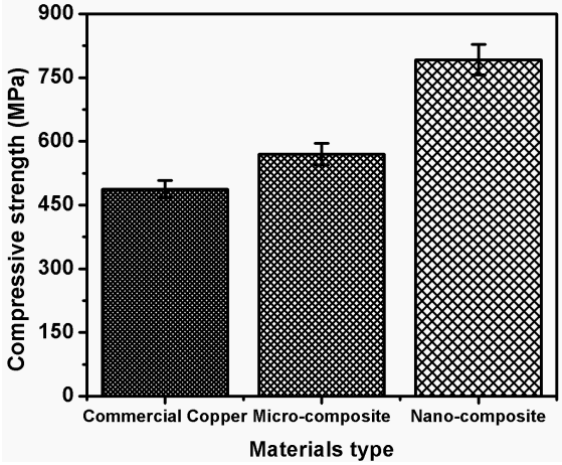

Figure 8. Compressive strengths of copper and copper composites

3.5. Electrochemical impedance spectroscopy

Corrosion behaviors of copper and copper-WC composites in 0.5 M H_2SO_4 solutions are investigated by EIS technique and shown in Figure 9. It is observed through analysis of Figure 9 that corrosion resistance of copper is significantly increased by addition of ceramic WC powder particles as a filler material; however, maximum anticorrosion potential is shown by Cu-WC nano composite. Ceramic materials are well known for its high corrosion resistance. Hence, addition of ceramic WC particles in copper matrix increased resistance of composite material against acid corrosion. Furthermore, fine distribution of WC nano particles in copper matrix enhanced the interaction points (area) between WC particles and copper molecules, which resulted in high strength of Cu-WC nano composite. This fact is clearly manifested in corrosion test, which is in good agreement with Vickers hardness test and compression test. Further analysis of impedance data via Bode plots (Figure 10) revealed that phase angle for copper is lower than that of copper composites. In other words, it could be said that phase angle was closer to 90° for Cu-WC composites with respect to copper, which is the artifact of higher corrosion resistance of Cu-WC composites in sulfuric acid solutions.

To obtain more details from impedance curves, Nyquist plots are fitted with an equivalent electrical circuit (EEC) as shown in Figure 11 [33-35]. The different elements of EEC could be described as: solution resistance, R_s; charge transfer resistance, R_t; and constant phase element,

CPE. Nyquist plots of copper and copper matrix composites showed that corrosion process is governed by charge transfer reactions only (one time constant). However, the shape of impedance spectra is not semicircular; CPE is used to show modified capacitor behavior of electrodes in sulfuric acid solutions.

A quick analysis of Table 1 revealed that impedance of copper against corrosion in sulfuric acid solution increased due to alloying with WC particles. However, Cu-WC nano composite showed more corrosion resistance than Cu-WC micro composite. The first reason for this fact could be extracted from the changes in "n" values. Table 1 showed that there is increase in "n" values when nano sized WC particles are used to make copper matrix composites instead of micro sized WC particles. This means that surface properties of the electrode is modified in a better way in presence of nano WC particles, which could also be observed in bode phase angle plots (Figure 10). The second reason could be given as decrease in CPE values. On immersion of working electrodes in electrolyte solution, corrosion products are formed at the interface. These corrosion products (preferably oxides) acted as a medium having one side copper and copper matrix composite electrodes and electrolyte on other side, equivalent to two plates of a capacitor. A decrease in capacitance might correspond to: increase in the thickness; or decrease in dielectric constant; or decrease in porosity of protective corrosion products layer formed at electrode-acid interface [36-39], which resulted in high corrosion resistance of Cu-WC nano composite.

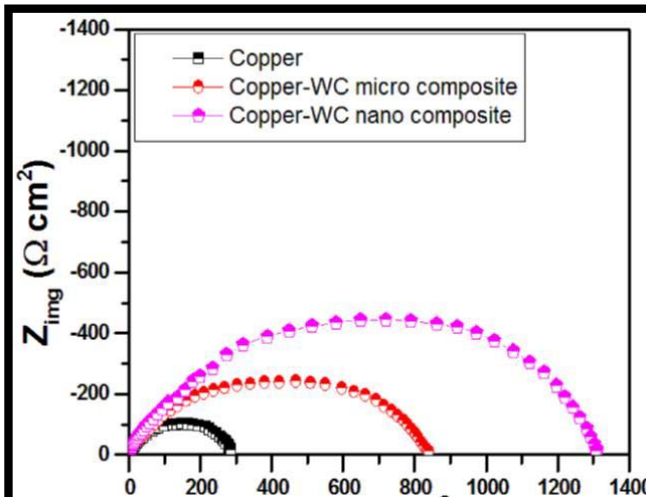

Figure 9. Nyquist Plots for Copper and Copper composites in 0.5 M H_2SO_4 solutions

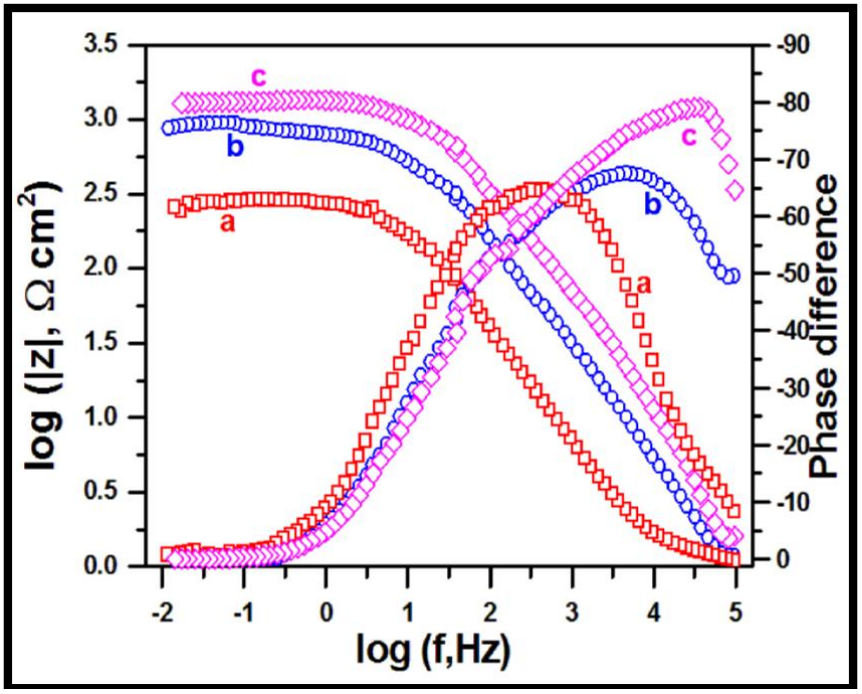

Figure 10. Bode Plots for Copper (a), Cu-WC micro composite (b) and Cu-WC nano composite (c) in 0.5 M H_2SO_4 solutions

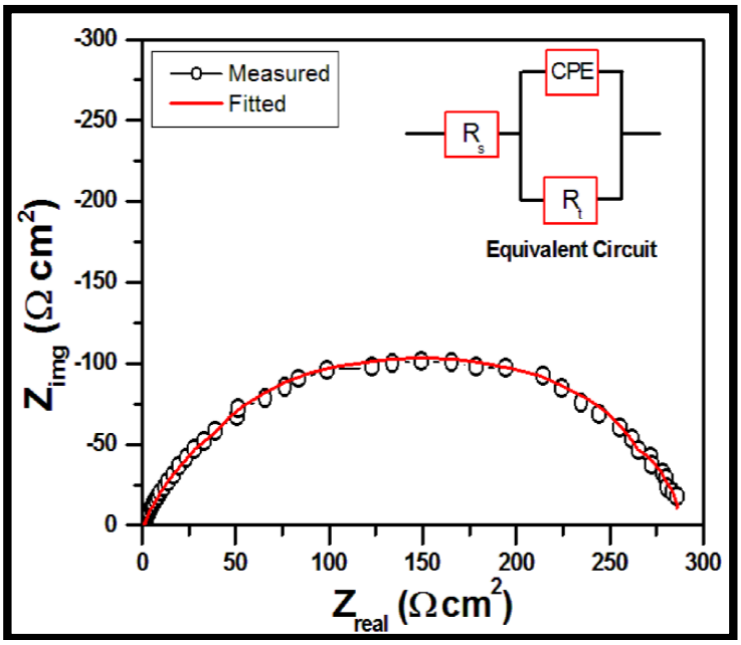

Figure 11. Electrochemical circuit and fitting of Nyquist Curves

Table 1. Technical Parameters obtained from Nyquist Plots for copper and copper composites in 0.5 M H_2SO_4 solutions at room temperature

S. No.	Materials	R_s (Ω cm^2)	R_t (Ω cm^2)	n	CPE (μF cm^{-2})
1-	Copper	1.06	285	0.801	108.50
2-	Cu-WC micro composite	0.34	845	0.821	34.45
3-	Cu-WC nano composite	1.10	1310	0.832	9.94

The corrosion study of copper and copper-WC composites clearly suggested that WC particles reinforce the corrosion resistance of copper in 0.5 M H_2SO_4 solution. Similar information is achieved by the surface morphology analysis of the unexposed and the exposed samples. A careful analysis of Figure 12 suggests that there is an inherent oxide layer on the surfaces of unexposed samples, which formed probably due to interaction of the samples with open air. Yet, the samples show smooth surfaces. On the other hand, the samples exposed in sulfuric acid illustrated a clear change in the surface morphology with respect to the unexposed samples. Figure 13 reveals that the greatest surface damage occurred in copper specimen; however, the copper-WC composites show just a slight degradation of the surface in sulfuric acid solution. Thus, it could be stated based on surface images that WC particles significantly enhanced the corrosion resistance of copper.

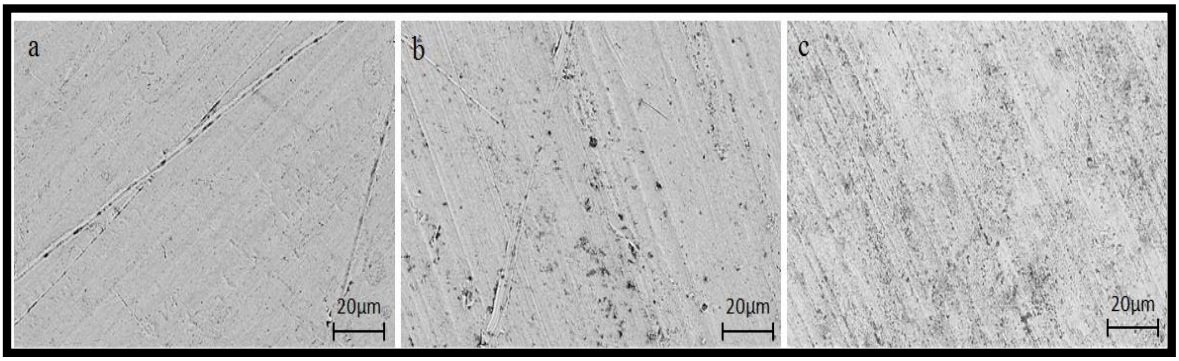

Figure 12. SEM images of unexposed **(a)** copper, **(b)** Cu-WC micro composite, **(c)** Cu-WC nano composite

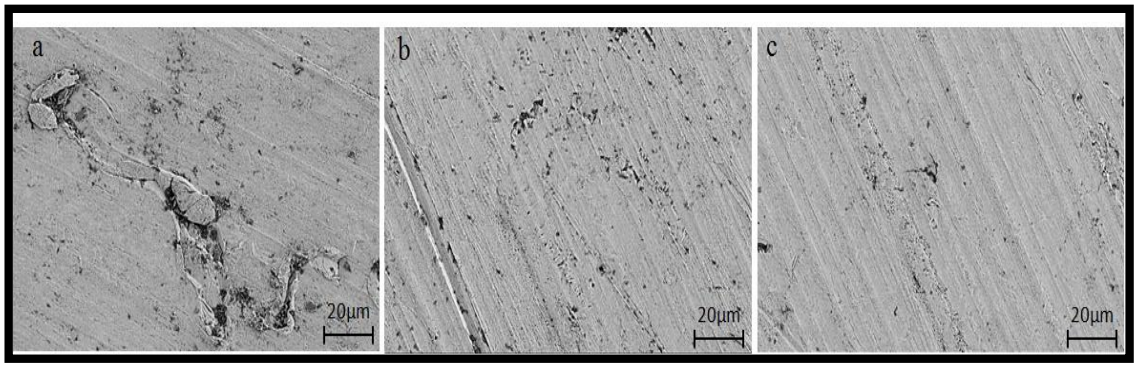

Figure 13. SEM images of exposed **(a)** copper, **(b)** Cu-WC micro composite and **(c)** Cu-WC nano composite in 0.5 M H_2SO_4 solutions for 2 hours

3.6 Overall comparison between copper and copper-WC composites

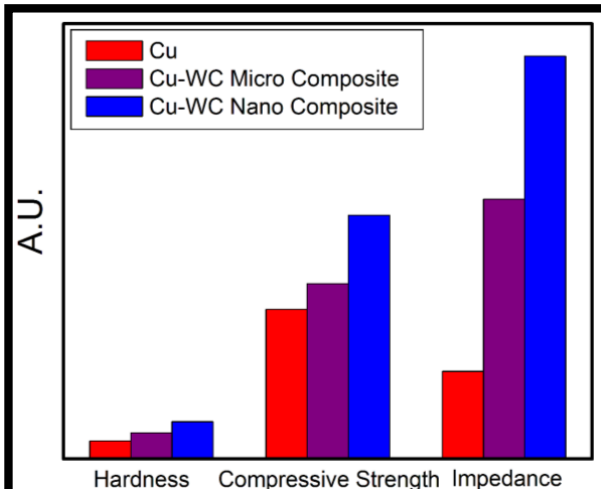

Figure 14. Comparison of mechanical and corrosion behavior of Cu and Cu-WC composites

Figure 14 shows an overall comparison of hardness, compressive strength and corrosion resistance values of copper and copper composites. It could be stated based on Figure 14 that mechanical and corrosion behavior of copper significantly improved due to reinforcement of WC particles. In addition, the comparison between Cu-WC micro composite and Cu-WC nano composite suggested that size of WC particles played a vital role in the improvement of the properties of copper. Due to decrease in size of the reinforcing WC particles, this caused better interaction between matrix and filler martial. Thus, the mechanical properties and corrosion behavior of Cu-WC nano composite became better that Cu-WC micro composite.

4. Conclusions

We prepared copper, Cu-WC micro composite and Cu-WC nano composite by stir casting technique in present study. The prepared copper and copper composites are characterized by XRD analysis, which confirms the formation of Cu-WC composites. Hardness and compressive strength of the test samples are estimated by Vickers hardness tester and universal testing machine. It is found from the results that hardness and compressive strength of Cu-WC composites are greater than that of copper matrix. Furthermore, anticorrosion strengths of cast copper and copper composites are tested in 0.5 M H_2SO_4 solutions, which show that copper composites are having higher corrosion resistance in comparison to alone copper. It could be concluded based on the results of various techniques that Cu-WC nano composite performed very well in all the tests followed by Cu-WC micro composite and copper respectively. Composite formation due to fine dispersion of WC particles in copper matrix could be given as the reason of above-mentioned fact.

5. References

[1] Michael S, Ralf F, Roman B 2011 Wiley-VCH, 1st Edition.
[2] Andrew D, Tsukrov I, Judson D, Aufrecht J, Adolf G and Hofmann U 2013 *Corros. Sci.* **76** 453–464.
[3] Youdi G, Zhou Z, Sizhe N, Ge W and Wang Y 2013 *J. Non-Cryst. Solids* **380** 135–140.
[4] Zhao H, Liu L, Wu Y and Hu W 2007 *Comp. Sci. and Tech.* **67** 1210–1217

[5] Lopez M, Corredor D, Camurri C, Vergara V and Jimenes J 2005 *Mater. Charact.* **55** 252–262.
[6] Suzuki S, Shibutani N, Mimura K, Isshiki M and Waseda Y 2006 *J. Alloy Compd.* **417** 116 – 120.
[7] Wong P K, Kwok C T, Man H C and Cheng F T 2012 *Corros. Sci.* **57** 228–240.
[8] Kwok C T, Lo K H, Chan W K, Cheng F T and Man H C 2011 *Corros. Sci.* **53** 1581–1591.
[9] Naka M, Hashimoto K and Masumoto T 1978 *J. Non-Cryst. Solids* **30** 29–36.
[10] Diard J P, Le J M C, Le B G and Montella C 1998 *Electrochim. Acta* **43** 2485–2501
[11] Wu T F, Qiu Z W, Lee S L, Lee Z G and Lin J C 2004 *Corros Eng Sci Tech.* **39** 229–235.
[12] Chouvy C D, Ammellot F and Sutter E M M 2001 *Appl. Surf Sci* **174** 55–61.
[13] Palumbo G, Aust K T and Erb U 1996 *Mater Sci Forum* **225** 281–286.
[14] Burstein G T and Gao G 1994 *J Electrochem. Soc.* **141** 912–921.
[15] Karpagavalli R and Balasubramaniam R 2007 *Corros. Sci.* **49** 963–979.
[16] Souissi N, Sidot E, Bousselmi L, Triki E and Robbiola L 2007 *Corros.Sci.* **49** 3333–3347.
[17] Robbiola L, Tran T T M, Dubot P, Majerus O and Rahmouni K 2008 *Corros. Sci.* **50** 2205–2215.
[18] Uddin S M, Mahmud T, Wolf C, Glanz C, Kolaric I, Volkmer C, Höller, Wienecke U, Roth S and Fecht H J 2010 *Composites Science and Technology* **70** 2253–2257.
[19] Simchi A and Godlinski D 2008 *Scripta Mater*. **59** 199-202.
[20] Wang F, Mei J and Wu X H 2007 *Mater. Design* **28** 2040-2046.
[21] Gu D D and Shen Y F 2008 *Appl. Surf. Sci.* **254** 3971-3978.
[22] Gu D, Shen Y and Lu Z 2009 *Mater. Design* **30** 2099-2107
[23] Ji G, Shukla S K, Dwivedi P, Sundaram S, Ebenso E E and Prakash R 2012 *Int. J. Electrochem. Sci.* **7** 12146-12158.
[24] Ji G, Shukla S K, Dwivedi P, Sundaram S, Ebenso E E and Prakash R 2012 *Int. J. Electrochem. Sci.* **7** 9933-9945.
[25] Singh A K, Ji G, Prakash R and Ebenso E E 2013 *Int. J. Electrochem. Sci.* **8** 9442 – 9448.
[26] Zhong Y, Ping D, Song Z and Yin F 2009 *J. Alloys Comp.* **476** 113-117
[27] Scherrer P 1918 *Nachr Ges Wiss Goettingen, Math-Phys Kl.* pp 98-100.
[28] Aung N N and Zhou W 2002 *J. Appl. Electrochem.* **32** 1397–1401.
[29] Zhang Z and Chen D L 2008 *Mat. Sci. Eng. A* **483** 148–152.
[30] Zhang Z and Chen D L 2006 *Scripta Mater.* **54** 1321–1326.
[31] Zadeh S A 2012 *Mat. Sci.Eng. A* **531** 112–118.
[32] Warraky E, Shayeb H A E and Sherif E M 2004 *Anti-Corros. Method M,* **51** 52–61.
[33] Ji G, Shukla S K, Dwivedi P, Sundaram S and Prakash R 2011 *Ind. Eng. Chem. Res.* **50** 11954-11959.
[34] Ji G, Dwivedi P, Sundaram S and Prakash R 2013 *Ind. Eng. Chem. Res.* **52** 10673-10681
[35] Ji G, Dwivedi P, Sundaram S and Prakash R 2015 *Res. Chem. Inter.* DOI: 10.1007/s11164-015-2029-y
[36] Ji G, Anjum S, Sundaram S and Prakash R 2015 *Corros. Sci.* **90** 107-117
[37] Doner A, Yuce A O and Kardas G 2013 *Ind. Chem. Res.* **52** 9709-9718
[38] Zarrouk A, Hammouti B, Dafali A and Bentiss F 2013 *Ind. Chem. Res.* **52** 2560-2568
[39] Ji G, Shukla S K, Ebenso E E and Prakash R 2013 *Int. J. Electrochem. Sci*. **8** 10878-10889.